CALCULATION OF THE TEMPERATURE FIELD OF A BAR FOR HARDENING IN A WATER-COOLED CRYSTALLIZING TANK

N. A. Avdonin, L. A. Volokhonskii, G. F. Ivanova, and A. L. Tsikerman

UDC 536.421.4

A mathematical model is given describing the heat field in vacuum-arc melting. A numerical computational method is described and the results of actual computations on a digital computer are given.

At the present time the industrial production of high quality metals by melting in a water-cooled crystallizing tank is widely practiced. Very frequently vacuum-arc melting furnaces are used. The main outline of the process is shown in Fig. 1.

Melting begins when the first drops of liquid metal fall on a layer of cold metal of given thickness (the so-called templet). The metal drops also fall on the wall of the crystallizing tank and congeal on it, forming with the condensate the so-called "corona." As the flowing electrode fuses, the bar grows and, as a result of thermal shrinkage as it cools, it branches out from the wall, forming a thermal gap, through which radiative heat transfer occurs (the region Γ_{1t}).

Under the mirror of the bath (Γ_{2t}) and also at the water-cooled tray (Γ_{0t}) there is direct contact between the bar and the wall; heat transfer in these regions may be radiative or by thermal conductivity. In this connection, it is more convenient for the ensuing discussion to assume that in this case the heat transfer is determined by Newton's law with a certain equivalent-contact heat-transfer coefficient α_c. The numerical values of the heat-transfer coefficients α_2 and α_0 between the bar and the wall of the crystallizing tank in the region Γ_{2t} and between the bar and the tray in the region Γ_{0t} respectively were determined experimentally in the furnaces used by the method of separate calorimetric measurements and also by the direct measurement of the wall temperature of the crystallizing tank.

Radiation occurs from the mirror of the liquid-metal bath (region Γ_{3t}) in the gap between the wall and the electrode and at the electrode, the temperature of the end of which can be taken as constant, equal to T_e. In addition, the mirror of the bath absorbs part of the heat emitted in the arc.

The process of forming the bar is nonstationary. At the initial moment of fusion, when the cooling effect of the tray is important, the liquid-metal lune is flat. As fusion continues the lune deepens until the onset of quasistationary thermal conditions.

An important problem in the study of the formation of the bar is the determination of the thermal field of the bar, and in particular, the position and shape of the crystallization isothermal. By studying the relation between the thermal field and the parameters of the process it is possible to make important conclusions about the optimal course of the process.

But experimental measurement of the thermal field is almost unattainable because of the difficulty of access to the working region of the furnace and the great complexity in the measurement of the temperature of the liquid metal.

In formulating the problem we make the following assumptions:

1) the heat in both the solid and liquid phases is conducted only by thermal conductivity;

Petra Stuchki Riga State University, All-Union Scientific Research Institute of Electrothermal Equipment, Moscow. Translated from Inzhenerno-Fizicheskii Zhurnal, Vol. 18, No. 1, pp. 124-132, January, 1970. Original article submitted February 6, 1969.

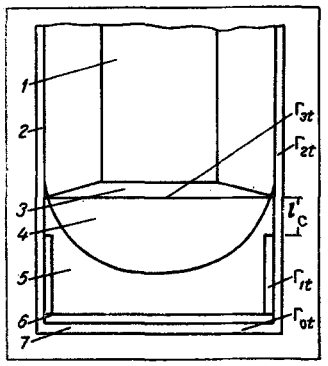

Fig. 1

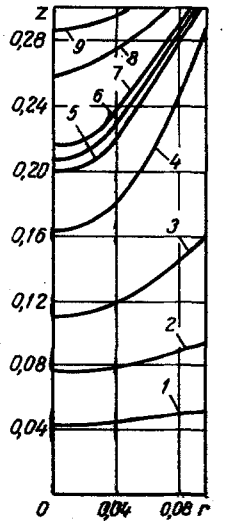

Fig. 2

Fig. 1. Diagram of a vacuum-arc furnace: 1) test electrode; 2) water-cooled crystallizing tank; 3) inter-arc gap; 4) liquid-metal lune; 5) hardening metal; 6) water-cooled tray.

Fig. 2. The isothermal field in the bar after 25 min melting: R = 0.095 m; T_m = 1700°C; r, m; z, m. 1) T = 500°C; 2) 700°C; 3) 900°C; 4) 1200°C; 5) 1570°C; 6) 1640°C; 7) 1700°C; 8) 1900°C; 9) 2100°C.

2) the rate v at which the bar fuses is constant;

3) at the boundary between the liquid and the solid phases liberation of the latent heat of crystallization is taken into account (Stefan's condition);

4) at the boundaries between the bar and the crystallizing tank and also at the surface of the bath of metal there is either heat exchange with the medium of known temperature or there is radiation.

Since the fused bar is cylindrical, we introduce a cylindrical coordinate system (r, z) with the origin at the point of intersection of the axis of the bar and the tray, the z-axis being directed upwards and the r-axis along the radius of the bar.

Let D_t be the region determined by the conditions

$$D_t = \{0 < r < R;\ 0 < z < L + vt\},$$
$$\Gamma_t = \sum_{i=0}^{3} \Gamma_{it}, \tag{1}$$

where Γ_t is the boundary of the system consisting of the following parts:

$$\begin{aligned} \Gamma_{0t} &= \{0 < r < R;\ z = 0\},\\ \Gamma_{1t} &= \{r = R;\ 0 < z < L + vt - l_c\},\\ \Gamma_{2t} &= \{r = R;\ L + vt - l_c < z < L + vt\},\\ \Gamma_{3t} &= \{0 < r < R;\ z = L + vt\}. \end{aligned} \tag{2}$$

The mathematical problem of determining the temperature field of the bar in the above physical process can be formulated thus: it is required to find the temperature distribution function T(r, z, t) which is the solution of the problem (3)-(6):

$$\operatorname{div}\left(k(T)\operatorname{grad}T\right) = c(T)\rho\,\frac{\partial T}{\partial t},\quad P(r, z) \in D_t,\ t > 0,\ T(r, z, t) \neq T_m, \tag{3}$$

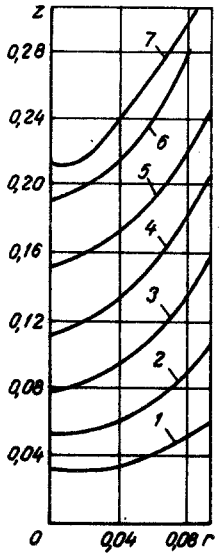

Fig. 3

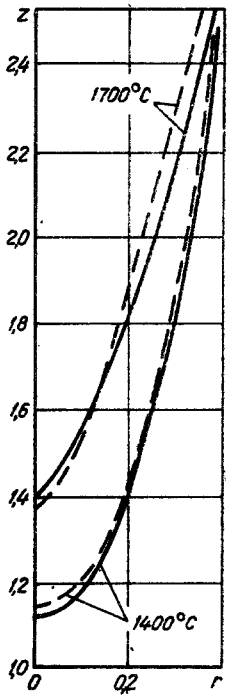

Fig. 4

Fig. 3. Position of the crystallization isothermal T_m = 1700°C with time; R = 0.095 m; r, m; z, m. 1) t = 2.1 min; 2) 6.2 min; 3) 10.4 min; 4) 14.6 min; 5) 18.7 min; 6) 22.9 min; 7) 25 min.

Fig. 4. Influence of the effective thermal conductivity of the liquid-metal k, on the position of the crystallization isothermal; R = 0.0435 m; r, m; z, m; the continuous line refers to k = 250 kcal/m · h · °C; the dotted to k = 25 kcal/m · h · °C.

$$\gamma\rho \frac{\partial \Phi}{\partial t} + ([k(T) \operatorname{grad} T], \operatorname{grad} \Phi) = 0, \; T(r, z, t) = T_m, \tag{4}$$

$$-k(T) \frac{\partial T}{\partial n} = F(T), \; P(r, z) \in \Gamma_t, \tag{5}$$

$$T|_{t=0} = T_0 < T_m. \tag{6}$$

Here $\Phi(r, z, t) = 0$ is the equation of the surface separating the liquid and solid phases; [grad T] is the discontinuity in grad T in passing through the surface $\Phi(r, z, t) = 0$ and

$$F(T) = \begin{cases} \alpha_0 (T - T_1), \; P(r, z) \in \Gamma_{0t}, \\ \varepsilon\sigma_0 \left[(T + 273)^4 - (T_2 + 273)^4\right], \; P(r, z) \in \Gamma_{1t}, \\ \alpha_2 (T - T_3), \; P(r, z) \in \Gamma_{2t}, \\ -q_1 + q_2 + q_3, \; P(r, z) \in \Gamma_{3t}, \end{cases} \tag{7}$$

where the T_i (i = 1, 2, 3) denote the temperatures of the external media on the parts Γ_{0t}, Γ_{1t}, Γ_{2t} of the boundary.

The heat flow at the boundary Γ_{3t} comprises:

1) the heat from the component arc (30% of all power)

$$q_1 = \frac{0.3\, IU}{F_0}; \tag{8}$$

2) the heat required to heat the drops of metal breaking away from the electrode at the superheat temperature to the temperature T at the surface of the metal bath:

$$q_2 = \frac{cG}{F_0}(T - T_e); \tag{9}$$

3) the heat radiated from the mirror of the metal bath to the electrode and in the gap between the wall of the crystallizing tank and the electrode,

$$q_3 = \begin{cases} \dfrac{\varepsilon}{2-\varepsilon}\sigma_0\left[(T+273)^4 - (T_e+273)^4\right], & 0 < r \leqslant R_{el}, \\ \varepsilon\cdot\sigma_0(T+273)^4, & R_{el} < r < R. \end{cases} \tag{10}$$

The problem (3)-(6), naturally, cannot be solved analytically because of the complexity of the boundary conditions, and also because of the nonlinearity of Stefan's condition. Hence the problem is solved numerically on a digital computer.

The problem (3)-(6) is the three-dimensional Stefan problem. For similar problems Oleinik [1] and Kamenomostskaya [2] have proved that there is a general solution and given a method for solving them numerically.

We make the change of variables

$$\vartheta = \int_{T_0}^{T} k(s)\,ds \tag{11}$$

and, following Oleinik and Kamenomostskaya, we introduce the function

$$a(\vartheta) = \int_0^{\vartheta} \alpha(s)\,ds + \beta\eta(\vartheta - \vartheta_1), \tag{12}$$

where $\alpha = (c\rho/k)$; $\vartheta_1 = \vartheta(T_m)$; $\beta = \gamma\rho$, and $\eta(x)$ is Heaviside's unit function,

$$\eta(x) = \begin{cases} 1, & x \geqslant 0, \\ 0, & x < 0, \end{cases} \tag{13}$$

and, using the smoothing method of Oleinik we replace the discontinuous function $a(\vartheta)$ by the differentiable function $a^*(\vartheta)$:

$$a^*(\vartheta) = \int_0^{\vartheta} c^*(s)\,ds, \tag{14}$$

where

$$c^*(\vartheta) = \begin{cases} \alpha(\vartheta), & 0 < \vartheta = \vartheta_1 - \delta, \\ \bar{\alpha}(\vartheta), & |\vartheta - \vartheta_1| < \delta, \\ \alpha(\vartheta), & \vartheta_1 + \delta \leqslant \vartheta, \end{cases}$$

$$\bar{\alpha} = \frac{\alpha(\vartheta_1 - \delta) + \alpha(\vartheta_1 + \delta)}{2} + \frac{\beta}{2\delta}.$$

Here $(\vartheta_1 - \delta, \vartheta_1 + \delta)$ is the smoothing interval for $a(\vartheta)$.

Thus, we pass from solving the problem (3)-(6) to determining the generalized solution of the following problem:

$$\frac{\partial^2\vartheta}{\partial r^2} + \frac{1}{r}\frac{\partial\vartheta}{\partial r} + \frac{\partial^2\vartheta}{\partial z^2} = c^*(\vartheta)\frac{\partial\vartheta}{\partial t}, \quad P(r, z) \in D_t, \; t > 0, \tag{15}$$

$$-\frac{\partial\vartheta}{\partial n} = F\left(T(\vartheta)\right), \quad P(r, z) \in \Gamma_t, \tag{16}$$

$$\vartheta|_{t=0} = 0. \tag{17}$$

For computational convenience we transform to nondimensional coordinates by putting

$$x=\frac{r}{R};\ y=\frac{z}{L+vt};\ \tau=\frac{t}{t^*};\ u=\frac{\vartheta}{\vartheta_1}. \tag{18}$$

Here $t^* = (L^* - L)/v$, where L^* is the finite length of the fused bar. Then conditions (15)-(17) can be rewritten as

$$a(x)\frac{\partial^2 u}{\partial x^2}+b(x)\frac{\partial u}{\partial x}+\bar{c}(\tau)\frac{\partial^2 u}{\partial y^2}+d(y,\ \tau,\ u)\frac{\partial u}{\partial y}=f(u)\frac{\partial u}{\partial \tau},\ 0<x,\ y,\ \tau<1, \tag{19}$$

$$\left.\frac{\partial u}{\partial x}\right|_{x=0}=0,\ \left.\frac{\partial u}{\partial x}\right|_{x=1}=\varphi(u)|_{x=1}, \tag{20}$$

$$\left.\frac{\partial u}{\partial y}\right|_{y=0}=\psi(u,\ \tau)|_{y=0},\ \left.\frac{\partial u}{\partial y}\right|_{y=1}=-\psi(u,\ \tau)|_{y=1}, \tag{21}$$

$$u|_{\tau=0}=0, \tag{22}$$

where

$$a(x)=\begin{cases}1, & x\neq 0,\\ 2, & x=0,\end{cases}\quad b(x)=\begin{cases}\dfrac{1}{x}; & x\neq 0,\\ 0; & x=0,\end{cases}$$

$$\bar{c}(\tau)=\frac{R^2}{(L+vt^*\tau)^2},\ f(u)=\frac{R^2}{t^*}c^*(\vartheta(u)),$$

$$d(y,\ \tau,\ u)=\frac{vt^*yf(u)}{L+vt^*\tau},\ \varphi(u)=-\frac{R}{\vartheta_1}F(T(\vartheta(u))),$$

$$\psi(u,\ \tau)=\frac{L+vt^*\tau}{\vartheta_1}F(T(\vartheta(u))).$$

To solve the problem (19)-(22) numerically we use the Peaceman–Rachford method of separating the two-dimensional problem into one-dimensional problems and solve the latter by one-dimensional trial runs.

We introduce a net with uniform steps δ_1, δ_2, δ_3 in the variables x, y, τ respectively and put

$$u(x_i,\ y_j,\ \tau_k)=u(i\delta_1,\ j\delta_2,\ k\delta_3)=u_{ij}^k.$$

We approximate Eq. (19) at time $\tau_{k+(1/2)}$ by the difference scheme

$$\begin{aligned}&a\frac{u_{i+1j}^{k+\frac12}-2u_{ij}^{k+\frac12}+u_{i-1j}^{k+\frac12}}{\delta_1^2}+b(x_i)\frac{u_{i+1j}^{k+\frac12}-u_{i-1j}^{k+\frac12}}{2\delta_1}\\ &+\bar{c}\left(\tau_{k+\frac12}\right)\frac{u_{ij+1}^k-2u_{ij}^k+u_{ij-1}^k}{\delta_2^2}+d\left(y_i,\ \tau_{k+\frac12},\ u_{ij}^k\right)\frac{u_{ij+1}^k-u_{ij-1}^k}{2\delta_2}\\ &=f(u_{ij}^k)\frac{u_{ij}^{k+\frac12}-u_{ij}^k}{\delta_3},\ i=1,\ 2,\ \ldots,\ n-1,\ j=1,\ 2,\ \ldots,\ m-1,\end{aligned} \tag{23}$$

and at time τ_{k+1} by the scheme

$$\begin{aligned}&a\frac{u_{i+1j}^{k+\frac12}-2u_{ij}^{k+\frac12}+u_{i-1j}^{k+\frac12}}{\delta_1^2}+b(x_i)\frac{u_{i+1j}^{k+\frac12}-u_{i-1j}^{k+\frac12}}{2\delta_1}+\bar{c}(\tau_{k+1})\frac{u_{ij+1}^{k+1}-2u_{ij}^{k+1}+u_{ij-1}^{k+1}}{\delta_2^2}\\ &+d\left(y_j,\ \tau_{k+1},\ u_{ij}^{k+\frac12}\right)\frac{u_{ij+1}^{k+1}-u_{ij-1}^{k+1}}{\delta_2}=f\left(u_{ij}^{k+\frac12}\right)\frac{u_{ij}^{k+1}-u_{ij}^{k+\frac12}}{\delta_3},\\ &i=1,\ 2,\ \ldots,\ n-1,\ j=1,\ 2,\ \ldots,\ m-1,\end{aligned} \tag{24}$$

while we approximate the boundary conditions (20)-(21) thus:

$$u_{0j}^{k+\frac12}=u_{1j}^{k+\frac12},\ j=1,\ 2,\ \ldots,\ m-1, \tag{25}$$

$$\frac{u_{nj}^{k+\frac{1}{2}} - u_{n-1j}^{k+\frac{1}{2}}}{\delta_1} = -\frac{R}{\vartheta_1}\,\varepsilon\sigma_0\left\{\left(T\left(\vartheta\left(u_{nj}^{k+\frac{1}{2}}\right)\right)+273\right)\right.$$

$$\left.\times\left(T\left(\vartheta\left(u_{nj}^{k}\right)\right)+273\right)^3 - (T_2+273)^4\right\},\ P(x,\ y)\in\Gamma_{1\tau}, \tag{26}$$

$$\frac{u_{nj}^{k+\frac{1}{2}} - u_{nj-1}^{k+\frac{1}{2}}}{\delta_1} = -\frac{R}{\vartheta_1}\,\alpha_2\left(T\left(\vartheta\left(u_{nj}^{k+\frac{1}{2}}\right)\right)-T_3\right),\ P(x,\ y)\in\Gamma_{2\tau}, \tag{27}$$

$$\frac{u_{i1}^{k+1} - u_{i0}^{k+1}}{\delta_2} = \frac{L+vt^*\tau}{\vartheta_1}\,\alpha_0\left(T\left(\vartheta\left(u_{i0}^{k+1}\right)\right)-T_1\right),\ P(x,\ y)\in\Gamma_{0\tau}, \tag{28}$$

$$\frac{u_{im}^{k+1} - u_{im-1}^{k+1}}{\delta_2} = -\frac{L+vt^*\tau}{\vartheta_1}\left\{-q_1+\frac{cG}{F}\left(T\left(\vartheta\left(u_{im}^{k+1}\right)\right)-T_e\right)\right.$$

$$\left.+p(x)\left[\left(T\left(\vartheta\left(u_{im}^{k+1}\right)\right)+273\right)\left(T\left(\vartheta\left(u_{im}^{k+\frac{1}{2}}\right)\right)+273\right)^3 - q(x)\right]\right\},$$

$$P(x,\ y)\in\Gamma_{3\tau},$$

where the $\Gamma_{i\tau}$ ($i = 0, 1, 2, 3$) denote the domains which the Γ_{it} ($i = 0, 1, 2, 3$) are transformed in passing to nondimensional coordinates, while the functions

$$p(x) = \begin{cases} \dfrac{\varepsilon}{2-\varepsilon}\,\sigma_0,\ 0 < x \leqslant \dfrac{R_{el}}{R}, \\ \varepsilon\sigma_0,\ \dfrac{R_{el}}{R} < x < 1, \end{cases}$$

$$q(x) = \begin{cases} (T_e+273)^4,\ 0 < x \leqslant \dfrac{R_{el}}{R}, \\ 0,\ \dfrac{R_{el}}{R} < x < 1 \end{cases}$$

are introduced to simplify the notation.

We calculate the temperature fields for titanium and steel bars by the method indicated. In one of the variants for titanium bars the following constants were used: R = 0.095 m, R_{el} = 0.06 m, I = 3.4 kA, U = 24 V, L* = 0.4 m, l_c = 0.072 m, G = 87 kg/h, v = 0.684 m/h, L = 0.02 m, ρ = 4500 kg/m^3, γ = 100 kcal/kg, T_m = 1700°C, T_e = 1775°C, ε_{liq} = 0.4, ε' = 0.7, α_0 = 2000 kcal/m^2·h·°C, α_2 = 850 kcal/m^2·h·°C and

$$k(T) = \begin{cases} 0.01475\,T + 7.525,\ T < T_m, \\ 25,\ T \geqslant T_m, \end{cases}$$

$$c(T) = \begin{cases} 0.11 + 0.19\cdot10^{-3}\,T - 0.1\cdot10^{-6}\,T^2,\ T < 1000\ °C, \\ 0.2,\ T \geqslant 1000\ °C. \end{cases}$$

For this variant the isothermal field after 25 min melting is shown in Fig. 2 and the movement of the isothermal $T = T_m$ as time passes is shown in Fig. 3.

An estimate of the value of the temperature of the metal bath can be obtained by putting the heat flow through the boundary Γ_{3t} equal to zero:

$$-k(T)\left.\frac{\partial T}{\partial n}\right|_{\Gamma_{3t}} = -q_1 + q_2 + q_3 = 0.$$

Making the change of variable x' = (T + 273)/100 and substituting the numerical value of the constant, we obtain we obtain a fourth-order equation for x', one of the roots of which is negative, two are complex and the fourth yields the approximate value T = 2200°C for the above variant, which agrees well with the results of the computer computation.

The results were also compared with those from the laboratory furnace. There was good agreement with experiment in the calculation of the maximum temperature under the electrode and also in the depth and shape of the liquid bath. Thus, the depth of the bath obtained from computations differed from that measured experimentally by 5-10%. The maximum bath temperature coincided to within 5%.

The degree of approximation of the computed data to the experimental data depends not only on the accuracy of the computations, but also on the accuracy with which the boundary conditions and the thermophysical constants are specified. The latter are usually measured during the experiment and are determined very approximately. The weakest point is the choice of the effective thermal conductivity of melting since there is almost no information about this in the literature and experimental determination of the coefficient is virtually impossible due to the complex convective motion in the liquid region. To verify the extent of the influence of the effective thermal-conductivity coefficient of the liquid metal on the temperature field of the bar, the problem was solved for a titanium bar with k between 25 and 250 kcal/m·h·°C. Figure 4 shows the 1400°C and 1700°C isothermals for a bar of diameter 870 mm in steady state conditions for k = 250 and 25 kcal/m·h·°C. The position of the crystallization front (T_m = 1700°C) varies little when k increases by an order of magnitude, although the temperature field itself in the liquid metal varied in such a way as to reduce the gradients. This makes it possible to say that some degree of convection in the liquid bath has little effect on the crystallization front shape.

The variants were computed on a BÉSM-2 computer.

The computed results and also their comparison with experimental data show that the mathematical model describing the fusion process in a vacuum-arc melting and the numerical method given can be used to study the melting process.

NOTATION

T_m	is the melting point;
T_e	is the electrode face temperature;
v	is the melting rate;
R	is the bar radius;
R_{el}	is the electrode radius;
L	is the templet thickness;
l_c	is the height of contact zone;
k(T)	is the thermal conductivity coefficient;
c(T)	is the specific heat capacity;
ρ	is the density;
γ	is the latent heat of melting;
σ_0	is Boltzmann's constant;
ε	is the degree of blackness;
α_2, α_0	are the heat transfer coefficients in Γ_{2t} and Γ_{0t} respectively;
I	is the current;
U	is the voltage;
F_0	is the area of bath mirror;
G	is the furnace output;
r, z, t, T	are the dimensioned coordinates;
x, y, τ, u	are the nondimensional coordinates.

LITERATURE CITED

1. O.A.Oleinik, Dokl.Akad.Nauk SSSR, 135, No.5 (1960).
2. S.L.Kamenomostskaya, High School Scientific Reports [in Russian], Vol.1, No.1 (1958).